

Molecular-Level Characterization of Asphaltenes Isolated from Distillation Cuts

Amy M. McKenna,^{*,†} Martha L. Chacón-Patiño,[†] Chad R. Weisbrod,[†] Gregory T. Blakney,[†] and Ryan P. Rodgers^{*,†,‡,§}

[†]National High Magnetic Field Laboratory and [‡]Future Fuels Institute, Florida State University, 1800 East Paul Dirac Drive, Tallahassee, Florida 32310-4005, United States

[§]Department of Chemistry and Biochemistry, Florida State University, 95 Chieftan Way, Tallahassee, Florida 32306, United States

S Supporting Information

ABSTRACT: Asphaltenes challenge nearly all analytical techniques because of their immense polydispersity in molecular composition and structure. This operationally defined fraction of crude oil, insoluble in *n*-alkanes but soluble in aromatic solvents, is known to concentrate in vacuum residues and is linked to fouling and deposition issues. However, presence and subsequent characterization of asphaltenes are seldom discussed in conventional/unconventional distillate fractions. Here, we isolate asphaltenes from conventional (<593 °C/1099 F) and unconventional (>593 °C) distillation cuts and provide molecular-level characterization by electrospray ionization and atmospheric pressure photoionization Fourier transform ion cyclotron resonance mass spectrometry as a function of boiling point. Our results indicate that asphaltene molecular composition starts in the vacuum gas oil range and extends into vacuum residues. Moreover, we report that distillable asphaltene composition exists as both highly polar (heteroatom rich), aliphatic (atypical asphaltenes) species as well as condensed aromatic structures (classical asphaltenes). As a function of distillation temperature, asphaltene compounds exhibit structural trends consistent with thermal cracking that starts between 510 and 538 °C, increases between 538 and 593 °C, and is readily observed at temperatures up to 700 °C. Above 600 °C, low molecular weight compounds (expected to boil at much lower temperatures) that are *n*-heptane insoluble are detected across all heteroatom classes. Results herein suggest that these compounds are formed through structural rearrangement of archipelago asphaltenes because of thermal cracking reactions that occur during distillation and precipitate as asphaltenes. We report the isolation and mass spectral characterization of asphaltenes isolated from distillation cuts and propose that quantification of asphaltenes in distillates is critical to predict and prevent problems related to catalyst deactivation.

INTRODUCTION

Asphaltenes are the fraction of crude oil that is insoluble in paraffinic solvents (e.g., *n*-heptane and *n*-pentane) and soluble in aromatic solvents (e.g., toluene and benzene) and comprise one of the most analytically challenging fractions of oil and thus, controversy continues over fundamental properties such as asphaltene molecular weight and structure.^{1–11} Undisputed, however, is this solubility-defined petroleum fraction's role in flow impedance in pipelines, deposition formation during crude oil transport, catalyst deactivation in refinery processes, well-bore plugging during oil recovery/transport, and water contamination during storage because of asphaltene stabilization of emulsions.^{12–16} Thus, the development of efficient methods to solve asphaltene-related problems will benefit from a molecular-level understanding of asphaltene composition and structure.^{17–19}

The bulk elemental composition of asphaltenes has been historically less controversial, with agreement that asphaltenes exhibit bulk H/C ratios between ~0.90 and 1.15.^{20–30} Asphaltene molecular weight was addressed in the work of Dickie and Yen³ and revised in the 1980s by Boduszynski, who demonstrated that petroleum aromaticity, molecular weight, and heteroatom content increases concurrently with boiling point,^{39–44} but remained highly controversial.^{37,38,45–48} Combined, these works with others that followed led

petroleum researchers to agree that asphaltene molecular weight ranges between ~250 and 1200 g/mol with an average of ~750 g/mol.^{9,31–38,49–54}

The definition of these enigmatic species, rooted in terms of their solubility properties rather than their molecular structure, imparts an intrinsic ultracomplexity to this problematic fraction. Isolation of asphaltenes from crude oil yields a polydispersed mixture that may exhibit over 50 000 different elemental compositions that are enriched in pericondensed aromatic structures and contain structural cores connected by aryl, alkyl/cycloalkyl bridges.^{7,8,53,55–61} The structural controversy of asphaltenes arises from the inconsistency between the island model and asphaltene pyrolysis/thermal cracking products but has recently been resolved by high resolution mass spectrometry and tandem MS experiments.^{5,32,59,62–67} Aromatic structures are more stable during thermal cracking reactions; therefore, the generation of low molecular weight products is indicative of the breakage of covalent bonds across more complex bridged structures, where aromatic cores are connected via alkyl-chains, biomarker-like bridges (cycloalkane rings), sulfides, esters, and aryl bridges.^{9,32,68–70} These cracked

Received: December 6, 2018

Revised: January 24, 2019

Published: January 24, 2019



products, along with island-type asphaltene structures, can undergo condensation reactions that lead to coke formation.⁷¹ Asphaltene structural motifs are of significant concern in the work presented herein, as unconventional, short path distillation temperatures exceed those in conventional refinery operations. As a result, thermal cracking products must be considered.

Asphaltenes accumulate in vacuum residues and have long been considered “nondistillable” due to inherently low volatility.^{72,73} However, Boduszynski challenged this assumption 30 years ago and demonstrated that “nondistillable” residues can be further fractionated on the basis of solubility and that a portion of the subfractions may exhibit a distillable nature.^{4,41–44} Moreover, Boduszynski et al. hypothesized that all nonaggregated petroleum compounds are soluble in heptane and concluded that asphaltenes were only insoluble due to aggregation.⁴ In other words, only the aggregates that result from cooperative and strong intermolecular interactions between the individual petroleum compounds exhibit insolubility in paraffinic solvents.⁴

Asphaltenes, widely known to cause catalyst deactivation, are coke precursors and contain higher concentrations of heavy metals (e.g., nickel and vanadium).^{74–79} Thus, the detection and characterization of asphaltenic species in high-boiling distillation cuts is critical for maximizing the yield of valuable refinery products and minimizing costs that arise from catalyst deactivation and sludge/sediment formation, which can cause deposition and plugging.⁶⁴

Here, we present the isolation, detection, and characterization of asphaltenes isolated from distillate fractions from three geographically unique crudes: South American extra-heavy crude (482–533 °C), Middle Eastern heavy crude (510–538 and 538–593 °C), and Mackay bitumen (550–600, 600–650, and 650–700 °C) and report the molecular characterization of two distinct types of “distillable asphaltenes” by Fourier transform ion cyclotron resonance mass spectrometry (FT-ICR MS).

■ EXPERIMENTAL METHODS

Sample Preparation. The Middle Eastern heavy oil was supplied by General Electric Global Research (Niskayuna, NY), and distillation was performed in a still pot as previously reported.⁸⁰ Distillation cuts from South American extra heavy crude (482–533 °C), Middle Eastern heavy crude (510–538, 538–593, and residue 593+ °C) Mackay bitumen (550–600, 600–650, 650–700, and 700+ °C), were fractionated into *n*-C₇ asphaltenes and C_{5–6} asphaltenes as noted below.^{7,8,81,82} High-performance liquid chromatography-grade *n*-heptane (*n*-C₇), *n*-pentane (*n*-C₅), and toluene (J.T. Baker Chemicals, Phillipsburg, NJ, U.S.A.) and Whatman #2 filter paper (30 μm, 150 mm diameter, GE Healthcare Bio-Sciences, Pittsburgh, PA, U.S.A.) were used as received. All samples were dissolved in toluene to produce a stock solution of 1 mg/mL and further diluted to 250 μg/mL in 25:75 methanol/toluene (vol/vol) methanol spiked with 2% (by volume) formic acid for positive-ion electrospray ionization (ESI) or 0.25% (by volume) tetramethylammonium hydroxide (25% by weight in methanol) for negative-ion ESI (250 μg/mL) or further diluted to 200 μg/mL in toluene for atmospheric pressure photoionization (APPI) FT-ICR mass spectral analysis unless otherwise noted.

Isolation and Purification of C₇ Asphaltenes and C_{5–6} Asphaltenes. Asphaltenes were isolated from distillation cuts and residues from South American crude (482–533 °C), Middle Eastern heavy crude (510–538 and 538–593 °C), and Mackay bitumen (550–600, 600–650, 650–700 °C) based on a modified ASTM D6560-12 method.⁸³ In brief, 400 mL of *n*-C₇ was added dropwise

(~60 min) to 10 g (bitumen) and to 20 g (Middle Eastern heavy) of each distillation cut under sonication, followed by reflux at 110 °C for 1 h. For the Mackay bitumen vacuum residue, 1000 mg of material was used. The mixtures were allowed to stand overnight. The *n*-C₇ insoluble material was recovered by filtration and Soxhlet extracted with *n*-heptane until the washing solvent was colorless. *n*-C₇ asphaltenes were recovered by dissolution in toluene and desolvated under dry nitrogen (N_{2(g)}) at room temperature. Asphaltenes were crushed and rewashed with hot *n*-heptane for additional purification to decrease the concentration of entrained/occluded maltenes (C₇-soluble). Additionally, *n*-C₅ asphaltenes were isolated from each distillate, which were then washed with *n*-heptane for 50 h to isolate the asphaltene fraction insoluble in *n*-C₅ and soluble in *n*-C₇, technically known as C_{5–6} asphaltenes. The samples were dried under N_{2(g)}, weighed, and stored in the dark to avoid photo-oxidation.

Linear Ion Trap Mass Spectrometry. Positive-ion APPI broadband mass spectra were acquired with a linear ion-trap mass spectrometer (Thermo-Fisher Scientific Inc., San Jose, CA, U.S.A.) under experimental conditions similar to those described below.

FT-ICR Mass Spectrometry and Data Analysis. Ions were generated at atmospheric pressure via an APPI source (Ion Max APPI source, Thermo-Fisher Scientific Inc., San Jose, CA, U.S.A.) or via micro electrospray.⁸⁴ All samples were analyzed by 9.4 T FT-ICR MS⁸⁵ and 21 T FT-ICR MS.^{86,87} The ions were initially accumulated in an external multipole ion guide (9.4 T: 50–500 ms, 21 T: 1–5 ms) and released *m/z*-dependently by decrease of an auxiliary radio frequency potential between the multipole rods and the end-cap electrode.⁸⁸ The ions were excited to *m/z*-dependent radius to maximize the dynamic range and number of observed mass spectral peaks (*m/z* 200–1500; 9.4 T: 25–47%, 21 T: 32–64%),⁸⁹ and excitation and detection were performed on the same pair of electrodes.⁹⁰ The seven-segment compensated open cylindrical ICR cell in the 9.4 T FT-ICR is operated with 0.75–1 V trapping potential,^{91,92} and the dynamically harmonized ICR cell in the 21 T FT-ICR is operated with 6 V trapping potential.^{85,93} Time-domain transients of 6.8 (9.4 T) and 4.2 (21 T) s were acquired with the Predator data station with 100 (21 T) to 300 (9.4 T) time-domain acquisitions averaged for all experiments.⁹⁴ For 21 T FT-ICR MS, the Predator data station handled excitation and detection only, which were initiated by a TTL trigger from the commercial Thermo data station.⁸⁷ Mass spectra were phase-corrected⁹⁵ and internally calibrated with a high-abundance homologous series based on the “walking” calibration method.⁹⁶ Experimentally measured masses were converted from the International Union of Pure and Applied Chemistry (IUPAC) mass scale to the Kendrick mass scale⁹⁷ for rapid identification of homologous series for each heteroatom class (i.e., species with the same C_{*c*}H_{*h*}N_{*n*}O_{*s*}S_{*s*} content, differing only by degree of alkylation).⁹⁸ For each elemental composition, C_{*c*}H_{*h*}N_{*n*}O_{*s*}S_{*s*}, the heteroatom class, type (double bond equivalents, DBE = number of rings plus double bonds to carbon, DBE = C - *h*/2 + *n*/2 + 1),⁹⁹ and carbon number, *c*, were tabulated for subsequent generation of heteroatom class relative abundance distributions and graphical relative-abundance weighted DBE versus carbon number images. Peaks with signal magnitude greater than 6 times the baseline root-mean-square noise at *m/z* 500 were exported to peak lists, and molecular formula assignments and data visualization were performed with PetroOrg software.¹⁰⁰ Molecular formula assignments with an error >0.5 ppm were discarded, and only chemical classes with a combined relative abundance of ≥0.15% of the total were considered.

■ RESULTS AND DISCUSSION

Asphaltenes Isolated from Distillation Cuts. Table 1 shows the geographic origin and distillation range for each distillation cut, its API gravity (when possible), and weight percent yield of C_{5–6} and C₇ asphaltenes.

Molecular Weight Distribution of Distillable Asphaltenes. Figure 1 shows the broadband positive-ion APPI LTQ mass spectrum for C₇ asphaltenes isolated from the 538–593 °C distillate of the Middle Eastern heavy crude oil at three

Table 1. Weight Percent for n -C₇ and n -C_{5–6} Asphaltenes Isolated from South American Extra Heavy, Middle Eastern Heavy, and Mackay Bitumen Distillates

geographic origin	distillation temperature (°C)	API gravity	mass yield (wt %) C _{5–6} asphaltenes	mass yield (wt %) C ₇ asphaltenes
South American	482–533	17.7		0.23
Middle Eastern heavy	510–538	15.6	0.04	0.55
Middle Eastern heavy	538–593	14.1	0.25	0.33
Mackay bitumen	550–600		0.30	0.04
Mackay bitumen	600–650		0.59	0.08
Mackay bitumen	650–700		1.1	1.15
Mackay bitumen	700 ^a		3.7	16.6

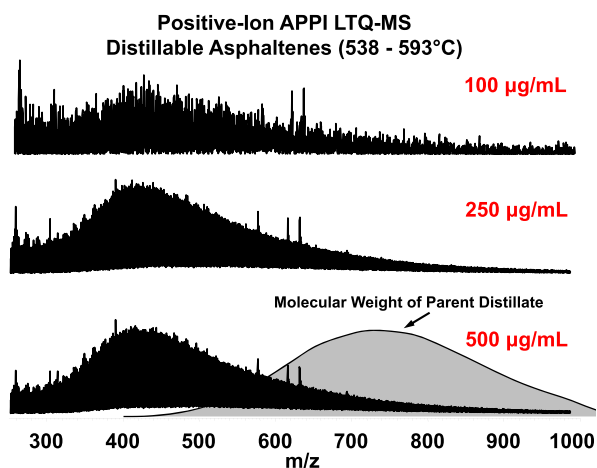


Figure 1. Broadband positive-ion APPI linear quadrupole ion-trap mass spectra of C₇ asphaltenes isolated from the 538–593 °C distillate of the heavy Middle Eastern crude oil at three different concentrations (100, 250, and 500 µg/mL). For reference, the molecular weight distribution for the parent distillate cut is shown in gray (bottom). The molecular weight distribution of the C₇ asphaltene species is clearly independent of concentration over the mass range analyzed and is roughly half the molecular weight of the parent distillate.

different concentrations (100, 250, and 500 µg/mL).⁸⁰ For reference, the molecular weight distribution for the parent distillate cut is shown in gray (bottom). The molecular weight distribution of the asphaltene species, which is not detected in the parent distillate (because of low concentration and selective ionization),⁷ is clearly independent of concentration and corresponds to roughly half the molecular weight of the parent distillate.⁸⁰ The Boduszynski continuum model states that petroleum composition is continuous in molecular weight and heteroatom content as a function of boiling point; therefore, compounds that are on the low end of the molecular weight distribution within a distillate cut must exhibit a higher content of O-, S-, and N-containing species and/or lower H/C ratios to remain in the same boiling point cut.^{41,42,80} Conversely, nonpolar hydrocarbons (HCs) with lower aromaticity (higher H/C) and lower heteroatom content must correspond to compounds with higher molecular weight in the same boiling point range.^{80,101} Thus, the asphaltenes isolated from this distillation cut must be enriched in heteroatoms and/or hydrogen deficient compounds relative to the maltenes from this distillation cut (discussed below).

Mass Defect and Spectral Complexity of Distillable Asphaltenes. Positive-ion ESI selectively ionizes basic

compounds in crude oil and is dominated by pyridinic nitrogen, which is the most abundant basic component of heavy crude.^{102–105} Asphaltenes exhibit higher heteroatom content and increased abundance of polyheteroatomic species compared to the parent oil and distillates. **Figure 2**

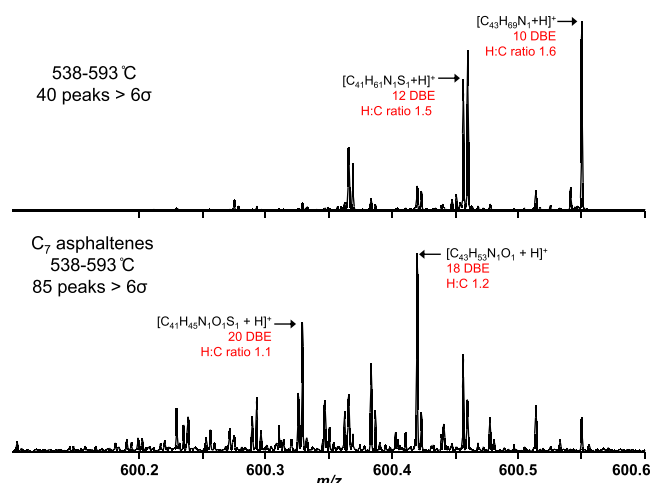


Figure 2. Zoom mass inset at m/z 600 for the parent 538–593 °C distillate (top) and corresponding C₇ asphaltene fraction (bottom) of the heavy Middle Eastern crude from positive-ion APPI FT-ICR mass spectra at 9.4 T. The C₇ asphaltene mass spectrum (bottom) contains more than twice the number of mass spectral peaks than the parent distillate cut across the same mass range, and asphaltene peaks are shifted to lower m/z (more hydrogen deficient and thus more aromatic or more heteroatoms per molecule) relative to the parent. The discovery of C₇ asphaltenes in distillate cuts supports the hypothesis that asphaltenes are continuous in class, type, and structure from low boiling to higher boiling fractions.

shows a mass-scale zoom inset at m/z = 600 for the 538–593 °C fraction of the Middle Eastern heavy crude (top) and its C₇ asphaltenes (bottom) and highlights the increased mass spectral complexity in distillate asphaltenes (**Figure 2**, bottom) when compared with the whole distillate (**Figure 2**, top). A shift to lower mass defect (0.10–0.55) in the asphaltene fraction occurs relative to the parent distillate (0.25–0.55) and indicates an increase in aromaticity and lower H/C ratio due to increased aromaticity of asphaltene core structures.⁸⁰ Specifically, the exact mass of hydrogen (¹H) is 1.007825 Da, whereas the exact mass of ¹²C is 12.00000 Da; therefore, the addition of one hydrogen atom to each compound (more aliphatic) increases the mass defect by +0.007825 Da. Saturated molecules have more hydrogen atoms and thus higher mass defects than aromatic compounds with the same nominal mass. For example, the two most abundant ions at m/z 600 in the parent distillate correspond to the protonated species C₄₃H₆₉N₁ with 10 DBE (H/C 1.6) and C₄₁H₆₁N₁S₁ with 12 DBE (H/C 1.5), whereas at the same nominal mass, the two most abundant asphaltene ions correspond to the protonated species C₄₃H₅₃N₁O₁ with 18 DBE (H/C 1.2) and C₄₁H₄₅N₁O₁S₁ with 20 DBE (H/C 1.1). Thus, the asphaltene fraction is composed of species that have an increase in heteroatoms and a decrease in hydrogen content, which shifts the peaks to a lower mass defect at every nominal mass detected. An increase in compositional complexity is evident in the asphaltene fraction, with more than twice the number of mass spectral peaks detected across the same mass range.

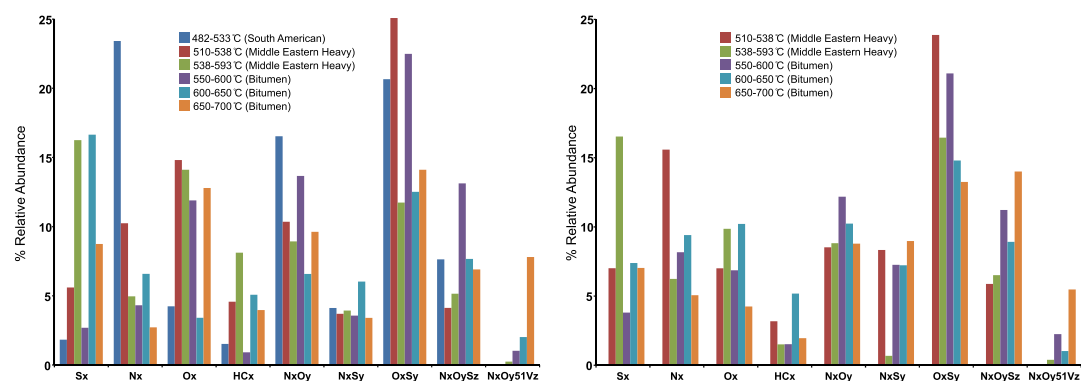


Figure 3. Summarized heteroatom class distribution for C₇ distillable asphaltene (a) and C₅₋₆ distillable asphaltene (b) derived from positive-ion APPI FT-ICR MS. HC denotes compounds that contain only carbon and hydrogen, and N₄O₁V₁ corresponds to the vanadyl porphyrins.

Asphaltenes at the Limit of Conventional Distillation.

C₇ Asphaltene Contains Both Aromatic and Aliphatic Structural Motifs. 482–533 °C South American Distillable C₇ Asphaltene. Compounds that report to the asphaltene fraction in the 482–533 °C distillate range span a wide range of heteroatom classes summed in Figure 3 (and shown also in Figure S1). APPI generates ions from nonpolar and polar compounds simultaneously, and both five-membered ring (pyrrolic) and six-membered ring (pyridinic) species are detected in a single mass spectrum.^{106,107} Thus, the N₁ class, as determined by APPI FT-ICR MS, includes both forms of aromatic nitrogen in petroleum (pyrrolic and pyridinic) plotted together as neutrals, although pyrrolic nitrogen tends to form protonated ions, whereas pyridinic nitrogen forms radical cations.¹⁰⁶ Figure 4 shows isoabundance-contoured plots of DBE (left) and H/C ratio (right) versus carbon number for the N₁, N₂, and NO₂ classes from *n*C₇ asphaltene isolated from the 482–533 °C distillate of South American crude. Relative-abundance weighted average DBE, H/C ratio, and carbon number are shown in red for each image. The most abundant N₁ compounds correspond to H/C ratio 1.0, indicative of a single, condensed aromatic core. Compounds that contain two nitrogen, which could be either pyridinic or pyrrolic, cover compositional space that increases in H/C with the increasing carbon number (Figure 3, right). A similar shift is noted for the NO₂ class (Figure 3, bottom), where the species span a wide range of H/C ratios (from 0.5 to 1.5). The trend strongly suggests that as the heteroatom content increases, the range of H/C ratios of the species that report to the asphaltene fraction widens.

Asphaltene Compositional Space Changes as Oxygen Content per Molecule Increases. C₇ asphaltene distilled between 482 and 533 °C contain a wide range of polyoxygenated compounds. Figure 5 shows the DBE versus carbon number images for S₁O_x classes. S₁ compounds are dominated by aromatic compounds (C₂₀–C₃₀) with DBE 19 (H/C ratio 1.0–1.2), and most likely correspond to thiophenic species, given the high DBE at a low carbon number and the high relative abundance at DBE = 15 (dinaphthothiophene) and higher ring number thiophenes. The S_xO_y classes (SO, SO₂, and SO₃) begin to shift to a lower DBE with the increased oxygen content. This “tipping over” in compositional space occurs with an increase in the heteroatom content, and the SO₂ and SO₃ classes are more aliphatic (lower DBE) than the S₁ and SO compounds. The H/C ratio gradually increases as a function of the oxygen content for S₁O_x (*x* = 0–3) classes: S₁, S₁O₁, S₁O₂, and (1.3) S₁O₃ translate to H/C ratios of 1.2, 1.3,

C₇-Asphaltenes Isolated from South American 482-533 °C Distillate

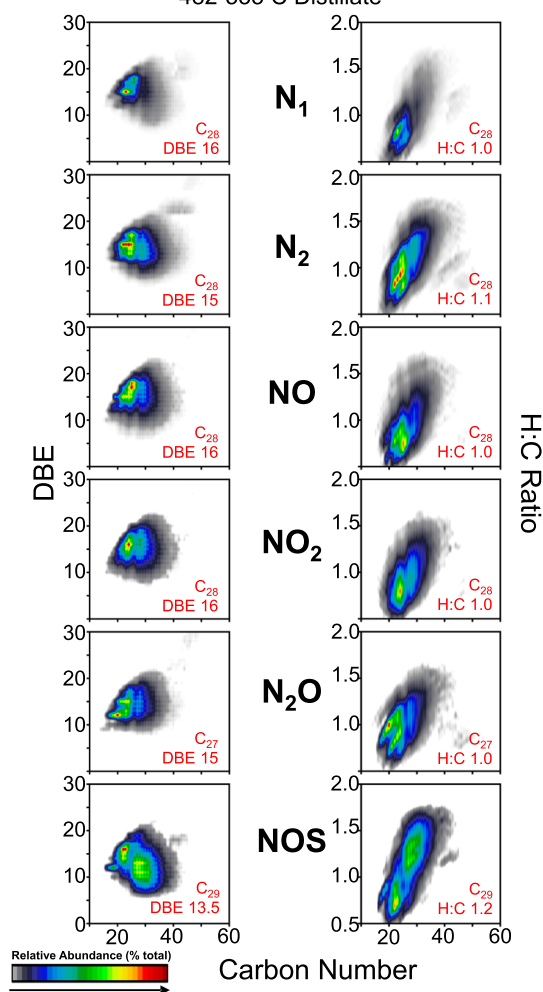


Figure 4. Isoabundance-contoured plots of DBE (left) and H/C ratio (right) vs carbon number for the six most abundant classes (N₁, N₂, NO, NO₂, N₂O, and NOS) obtained from positive-ion APPI FT-ICR MS of C₇ asphaltene isolated from the 482–533 °C distillate of the South American extra heavy crude. Relative-abundance weighted average DBE, H/C ratio, and carbon numbers calculated from neutral elemental compositions are shown in red for each heteroatom class.

1.4, and 1.4, respectively. The shift to lower DBE species with a concurrent increase in oxygen supports recent reports that asphaltene contains both classical (high DBE) compositions

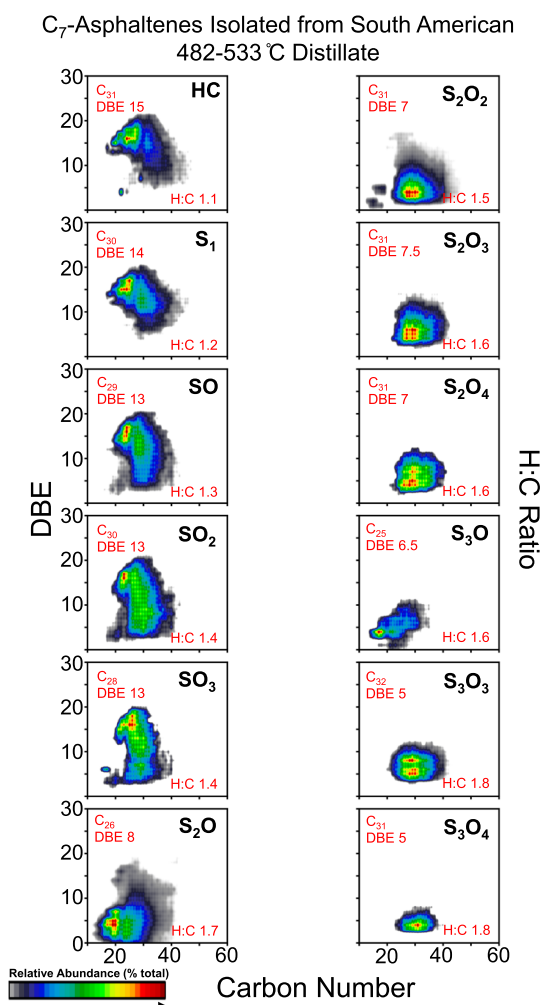


Figure 5. Isoabundance-contoured plots of DBE vs carbon number for 12 classes (HC, S₁, SO, SO₂, SO₃, S₂O, S₂O₂, S₂O₃, S₂O₄, S₃O, S₃O₃, and S₃O₄) obtained from positive-ion APPI FT-ICR MS of C₇ asphaltenes isolated from the 482–533 °C distillate of the South American extra heavy crude. Relative-abundance weighted average DBE, H/C ratio, and carbon numbers calculated from neutral elemental compositions are shown in red for each heteroatom class.

and atypical (low DBE with high content of O and/or S) species that span a continuum of chemical functionalities and structural motifs.^{7,8,108} The existence of aliphatic, low molecular weight asphaltenes that are enriched with oxygen and sulfur functionalities suggests that the asphaltene structural continuum begins in the vacuum gas oil (VGO)/heavy VGO (HVGO) distillates and given the cracked products detected at higher distillation temperatures as detailed further in the next section, suggests that they contain both archipelago and island moieties.^{7,8,109}

Asphaltenes at the Onset of Thermal Cracking. C₇ Asphaltenes in Middle Eastern Heavy Crude 538–593 °C Are Heteroatom Rich. The presence of heteroatom rich, aliphatic, and low molecular weight asphaltenes in the South American crude oil distillate (discussed above), in combination with the trend toward lower DBE values with increasing oxygen content, strongly suggests that oxygen chemical functionality is an important factor of asphaltene chemistry. However, these species were initially detected (Figure 4) by atmospheric pressure photo-ionization (APPI), which is known to preferentially ionize aromatic species. Thus, to

confirm the potential importance of oxygen chemical functionality for asphaltenes isolated from conventional distillation cuts, negative-ion ESI FT-ICR MS was employed, as ionization occurs through protonation/deprotonation reactions and selectively ionizes polar, acidic chemistries that are difficult to access by APPI.⁷ Figure S2 shows the heteroatom class distribution for the parent Middle Eastern heavy crude, the 538–593 °C distillate, and distillable C₇ asphaltenes extracted from the 538–593 °C distillate derived from negative-ion ESI FT-ICR MS. The most abundant classes in the parent oil and distillate contain ≤2 heteroatoms per molecule (HC, N₁, S₁, and N₁S₁), whereas distillable C₇ asphaltenes are enriched in polyoxygenated classes (e.g., O₄, S₁O₄, and S₂O₄).

Figure 6 shows the compositional progression for several acidic S_xO_y classes in 538–593 °C C₇ asphaltenes. H/C ratios range between 1.2 and 1.6 with stable core structures identified with the incorporation of each additional sulfur. S₁O₃ compounds span a bimodal distribution, with DBE values 1–25 and C₂₅–C₅₀. Addition of a second sulfur (S₂O₃) shifts the DBE distribution higher, and stable core structures can be identified at DBE 10 and 13, which strongly suggest that the second sulfur is thiophenic. Furthermore, a third sulfur (S₃O₃) shifts the DBE distribution even higher, with stable core structures at DBE 12 and 15. A similar trend is observed from S₁O₄ to S₃O₄. Although the changes in DBE with increased sulfur content are consistent with the additions of successive thiophenic sulfur structural motifs, they are concurrent with a shift downward in carbon number (Figure 6, top to bottom). Thus, despite their initial (and abnormally) aliphatic nature, these acidic, *n*-heptane insoluble compounds, isolated from a conventional distillate cut, obey the distillation rules set forth in the Boduszynski continuum model.^{20,110–112} Simply, their carbon number, DBE, and heteroatom changes are consistent with distillation. These results demonstrate the critical role of heteroatoms, specifically oxygen, in asphaltene behavior. Clear evidence of compositional trends that are inconsistent with the Boduszynski continuum model is noted at higher distillation temperatures.

Compositional Evidence of Thermal Cracking of Asphaltenes. Figure 7 shows DBE versus carbon number images for HCs, O₁, O₂, and O₃ classes for 510–538 °C (Figure 7a) and 538–593 °C (Figure 7b) C₇ asphaltenes from the Middle Eastern heavy crude. The planar aromatic limit is shown as a red dashed line on each image.^{113,114} Compounds at or near the planar limit correspond to condensed ring aromatics. A shift to higher carbon number and DBE occurs within a given heteroatom class from 510 to 538 °C. Asphaltenes between 510 and 538 °C correspond to primarily condensed ring systems for all heteroatom classes, with the most abundant compounds near or close to the planar limit line. However, as the temperature increases to 538–593 °C, low DBE (5 < DBE < 10) and low carbon number (~C₁₅–C₃₀) compounds are detected (highlighted by a white dashed oval). This strongly suggests that thermal cracking across bridged asphaltene structures occurs as the temperature approaches ~600 °C but starts at temperatures as low as 510–538 °C.

Direct comparison of the composition of HC, O₁, O₂, and O₃ classes of distillate asphaltenes indicates that asphaltenes are undergoing thermal cracking reactions that yield lower boiling, aliphatic compounds that remain *n*-heptane insoluble.¹¹⁵

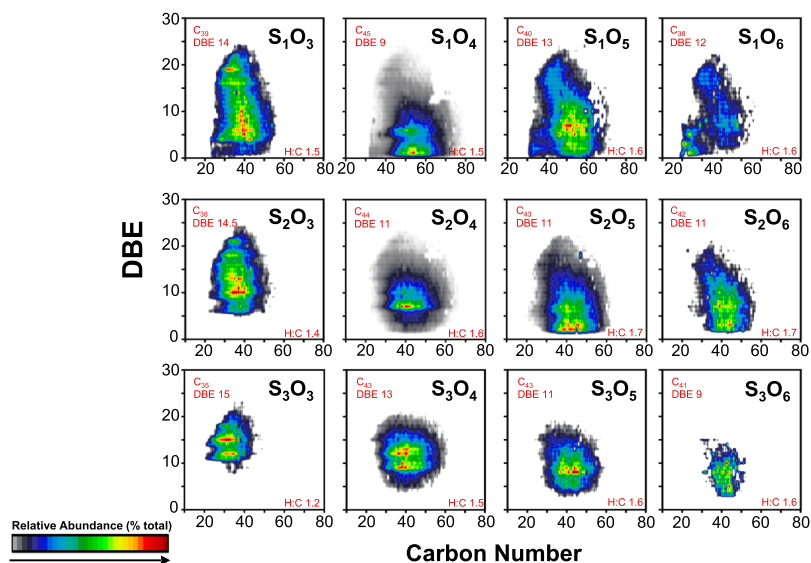
Acidic Species Derived from Negative ESI FT-ICR MS
 C_7 -insolubles Middle Eastern Heavy 538–593 °C


Figure 6. Isoabundance-contoured plots of DBE vs carbon number for S_xO_y classes obtained from negative-ion ESI FT-ICR MS of C_7 asphaltenes isolated from the 538–593 °C distillate of the heavy Middle Eastern crude. Relative-abundance weighted average DBE, H/C ratio, and carbon numbers calculated from neutral elemental compositions are shown in red for each heteroatom class.

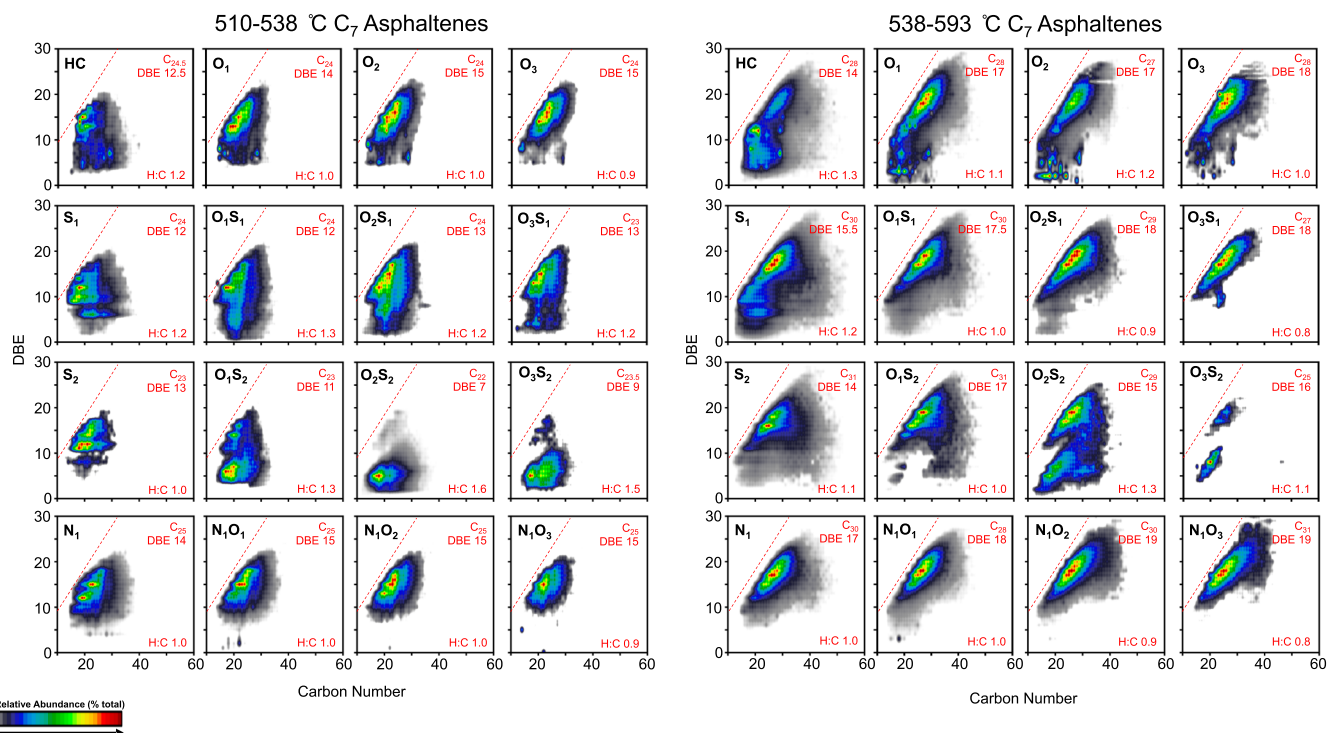


Figure 7. Isoabundance-contoured plots of DBE vs carbon number for 16 classes obtained from positive-ion APPI FT-ICR MS of C_7 asphaltenes isolated from the 510–538 °C distillate (A, left) and 538–593 °C distillate (B, right) of the heavy Middle Eastern crude. Relative-abundance weighted average DBE, H/C ratio, and carbon numbers calculated from neutral elemental compositions are shown in red for each heteroatom class.

Definitive Evidence of Thermal Cracking in Asphaltenes above 600 °C. *Thermal Cracking of C_7 Asphaltenes Yields Low Molecular Weight Compounds.* The Mackay bitumen was distilled in 50 °C increments, and the three highest boiling cuts (550–600, 600–650, and 650–700 °C) and its vacuum residue (700+ °C) were fractionated into C_7 and C_{5-6} asphaltenes. The bitumen was fractionated in such a manner because previous work suggests that archipelago

structural motifs are enriched in the C_7 asphaltene fraction, whereas island structures are enriched in the C_{5-6} fraction.^{7,8} Figure 8 shows DBE versus carbon number images for the four classes (HC, S_1 , O_1 and N_1) detected across all four boiling point ranges.

Asphaltenes between 550 and 600 °C. For C_7 asphaltenes in the 550–600 °C distillates, HCs and monoheteroatomic classes (S_1 , O_1 , and N_1) contain an average of C_{35} with DBE

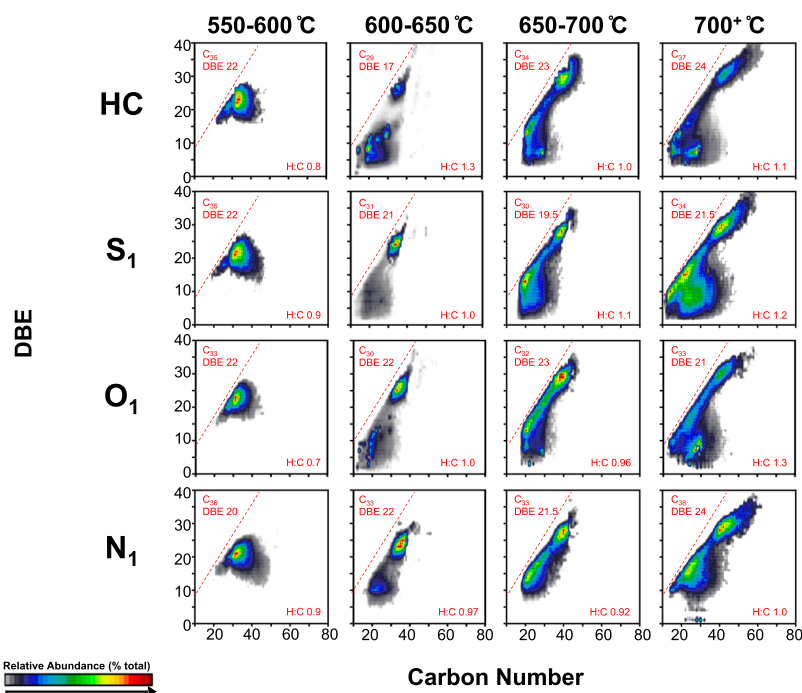


Figure 8. Isoabundance-contoured plots of DBE vs carbon number for four classes (HCs, S_1 , O_1 , and N_1) obtained from positive-ion APPI FT-ICR MS of C_7 asphaltenes isolated from 550 to 600, 600–650, and 650–700 °C distillates and the 700⁺ °C residue of the Mackay bitumen. Relative-abundance weighted average DBE, H/C ratio, and carbon numbers calculated from neutral elemental compositions are shown in red for each heteroatom class.

values of 20–22 that convert to the H/C ratio of 0.7–0.9, suggesting abundant condensed aromatic structures.⁵⁵ Asphaltenes within this fraction are close to the planar stability limit across a narrow carbon number range, with H/C ratios that correspond to condensed aromatic (island) structures.

Asphaltenes between 600 and 650 °C. Compositional evidence of thermal cracking is presented in asphaltenes from the 600–650 °C distillate. Across all classes, a bimodal distribution occurs with two distinct structural components. In the HC class, condensed aromatics are identified between C_{30} – C_{42} and C_{15} – C_{30} across DBE 4–15. These compounds are thermal degradation products generated by distillation above 600–650 °C and indicate the breaking of covalent bonds. These compounds are volatile at lower temperatures and would distill at lower temperatures and thus not be present in the 600–650 °C range unless formed during the distillation process itself. Importantly, both condensed aromatic and “cracked back” products report to the asphaltene fraction. A similar trend is observed for the S_1 , O_1 , and N_1 classes.

Asphaltenes between 650 and 700 °C. Above 650 °C, thermal degradation products begin to dominate the compositional space across all classes. Low molecular weight, low DBE asphaltene compounds are detected in nearly equal abundance as condensed aromatic structures at higher DBE values across all classes. For all classes, a clear bimodality exists between classical asphaltenes, with composition at or approaching the planar limit line.⁵⁵ Both low DBE (aliphatic) and high DBE (aromatic) species are observed across all classes, which indicates breaking of covalent bonds through thermal processes that create light, low boiling compounds.

Asphaltenes above 700 °C. Asphaltenes isolated from the 700⁺ °C residue clearly show compositional validation of thermal cracking. HCs with DBE 4–20 and carbon number < C_{40} are volatile at much lower temperatures and would be

volatile far below 700 °C, and thus not detected in the residue. These low molecular weight, atypical asphaltenes are formed through thermal degradation that occurs in the distillation process. Clear bimodality is observed in the HCs, S_1 , O_1 , and N_1 classes and agrees with previous results that C_7 asphaltenes are composed of a mixture of archipelago and island structural motifs.^{7,8} Extension to vacuum residue C_7 asphaltenes further supports the presence of two dominant structural motifs in asphaltenes based on the different slope for the higher DBE group (change in DBE/change in carbon number). This bimodality in structural motifs corresponds to island-type structures in the intermediate mass region (higher planar limit slope, hence higher degree of pericondensation) and archipelago-type structures in the higher mass region (lower planar limit slope, higher structural diversity).⁷ These low DBE, low carbon number compounds would not be present in the 700⁺ °C residue unless they were formed through cracking reactions that occur at high temperatures.

The Boduszynski Continuum Model Extends to asphaltenes. Both low DBE (more aliphatic) and high DBE (more aromatic) species are observed for S_1 , O_1 , and N_1 classes from 600 to 650 and 650–700 °C C_7 asphaltenes. This bimodality becomes more defined for 650–700 °C asphaltenes with the appearance of two groups of highly condensed, aromatic structures that approach the planar limit between C_{20} – C_{30} and C_{30} – C_{50} for all classes shown. Progression from 550 to 600 °C to the next highest distillate cut (600–650 °C) shifts the average carbon number in each class by 3–4 carbons and reveals a bimodal DBE and carbon number distribution for each class. This shift in relative abundance weighted average carbon number as a function of boiling point and heteroatom content agrees with the Boduszynski model.^{4,39,41–44} Detection of C_{15} – C_{30} compounds with DBE <15 in the same boiling point range as C_{30} – C_{40} compounds with DBE 25–30 indicates

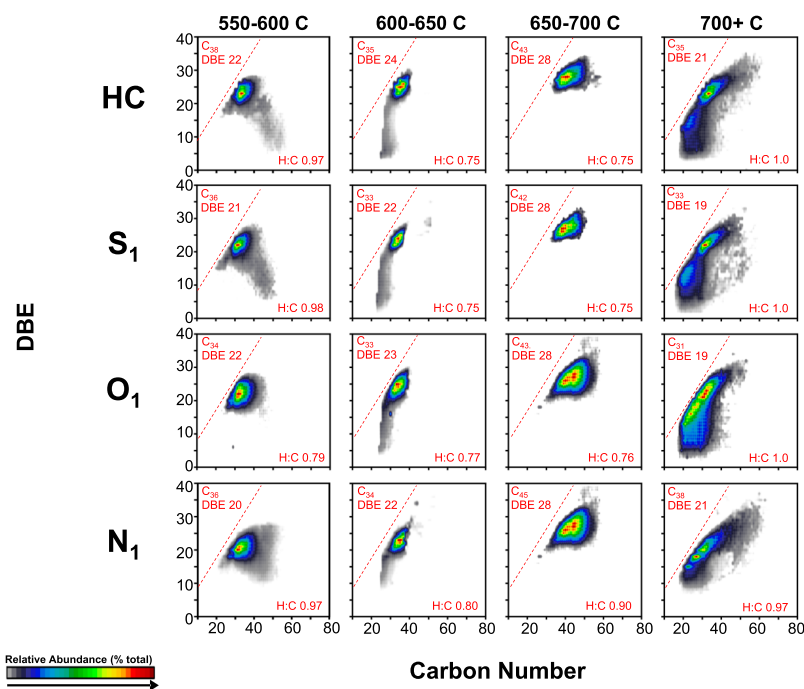


Figure 9. Isoabundance-contoured plots of DBE vs carbon number for four classes (HCs, S_1 , O_1 , and N_1) obtained from positive-ion APPI FT-ICR MS of C_{5-6} asphaltenes isolated from 550 to 600, 600–650, and 650–700 °C distillates and the 700+ °C residue of the Mackay bitumen. Relative-abundance weighted average DBE, H/C ratio, and carbon numbers calculated from neutral elemental compositions are shown in red for each heteroatom class.

both island and archipelago structural motifs. Moreover, vacuum residue C_7 asphaltenes contain definitive evidence that supports the presence of two dominant asphaltene structural motifs based on the different slope for the higher DBE group (change in DBE/change in carbon number) compared to 650–700 °C asphaltenes. This bimodality in structural motifs has recently been reported to correspond to island-type structures in the intermediate mass region (higher planar limit slope, hence higher degree of pericondensation) and archipelago-type structures in the higher mass region (lower planar limit slope, higher structural diversity).⁷ We predict that both archipelago and island-type structural motifs are present in C_7 asphaltenes in distillation cuts from the HVGO range to vacuum residues, and structural characterization based on tandem MS fragmentation patterns will be the subject of future studies. Regardless, the presence of abundant low DBE and low carbon number species, with boiling points much lower than the distillate cut in which they were detected, strongly suggests that they arise from thermally induced cracking of higher DBE and higher carbon number archipelago-type structures.

Island and Archipelago Structural Motifs Exist in Distillable Asphaltenes. C_{5-6} Asphaltenes Are Dominated by Island Structures. Figure 9 shows DBE versus carbon number images for C_{5-6} asphaltenes from the four bitumen-derived samples. C_{5-6} asphaltenes have lower H/C ratios compared to C_7 asphaltenes within the same class, which suggests that independent of solubility (C_5 -insoluble/ C_7 -soluble), these compounds are enriched in highly aromatic/alkyl deficient compounds that resemble the classical asphaltene structure.^{2,3} Unlike C_7 asphaltenes, C_{5-6} asphaltenes do not exhibit a high relative abundance of low molecular weight compounds below 700 °C. Thus, the majority of C_{5-6} compounds consists of a single core structure (island-type

asphaltenes), with little to no evidence of bimodal carbon number and DBE distribution. Progression to higher carbon number and DBE occurs with each successive boiling point, up to 700 °C, but the 700+ °C fraction has a lower DBE than the previous fraction, and cracking products are clearly evident. Thus, up to ~700 °C, the molecular level data suggests that C_{5-6} asphaltenes appear similar in heteroatom class distribution to C_7 asphaltenes and occupy similar compositional space. However, recent studies demonstrate that the main difference between C_{5-6} and C_7 asphaltenes is rooted in molecular structure.^{7,8} That difference is clearly evident in the number and relative abundance of thermal cracking products, which are obvious in the C_7 fraction but absent in the C_{5-6} fraction below 700 °C. Structural characterization through unimolecular fragmentation pathways inside the ICR cell will be the subject of future studies.

CONCLUSIONS

Historically, asphaltenes have been categorized as “nondistillables” thought to accumulate in vacuum residues. Herein, we identify *n*-heptane insoluble fractions (asphaltenes) in conventional and unconventional distillation cuts that exhibit bimodal distributions in carbon number and DBE space and indicate two dominant structural motifs (island and archipelago). Identification of compounds with low molecular weight and low carbon number distributions with boiling points above ~500 °C in asphaltenes isolated from three distinct crude oils indicates that thermal cracking of covalent bonds occurs across bridged structures present in asphaltenes. Thermal cracking reactions at or above ~600 °C yield compounds that should distill below the HVGO. Therefore, these compounds must be created after distillation occurs in the distillation process itself, otherwise they would be volatile and distill in lower fractions. Thus, “distillable asphaltenes” represent a class of molecules of

downstream concern, as asphaltene structure is rooted in the HVGO distillate range. Importantly, the compositional trends identified for “distillable asphaltenes” demonstrate that the molecular rules that govern petroleum distillation (Boduszynski continuum) also prevail in asphaltene chemistry. Moreover, the progression of the compositional space as a function of the increase in oxygen content suggests that intermolecular forces such as hydrogen bonding may play a critical role in asphaltene self-association. Future research will explore the evolution of the two main asphaltene structural motifs in distillate fractions to vacuum residues through fragmentation studies.

■ ASSOCIATED CONTENT

Supporting Information

The Supporting Information is available free of charge on the ACS Publications website at DOI: [10.1021/acs.energyfuels.8b04219](https://doi.org/10.1021/acs.energyfuels.8b04219).

Figures S1–S3 (PDF)

■ AUTHOR INFORMATION

Corresponding Authors

*E-mail: mckenna@magnet.fsu.edu. Phone: +1 850 644 4809. Fax: +1 850 644 1366 (A.M.M.).

*E-mail: rodgers@magnet.fsu.edu. Phone: +1 850 644 2398. Fax: +1 850 644 1366 (R.P.R.).

ORCID

Amy M. McKenna: [0000-0001-7213-521X](https://orcid.org/0000-0001-7213-521X)

Gregory T. Blakney: [0000-0002-4205-9866](https://orcid.org/0000-0002-4205-9866)

Ryan P. Rodgers: [0000-0003-1302-2850](https://orcid.org/0000-0003-1302-2850)

Notes

The authors declare no competing financial interest.

■ ACKNOWLEDGMENTS

The authors thank Christopher L. Hendrickson, Donald F. Smith, and John P. Quinn for design and maintenance of the 9.4 T and 21 T instruments and Yuri E. Corilo for software capabilities. The authors thank GE Global Electric Research in Niskayuna, NY for the Middle Eastern heavy distillates, Parviz Rahimi for the Mackay bitumen distillates, and Prof. Marianny Y. Combariza for the South American extra heavy crude. This work was supported by NSF Division of Materials Research through DMR-1157490 and DMR-1644779, and the State of Florida. A.M.M. and R.P.R. were partially supported by the Gulf of Mexico Research Initiative.

■ REFERENCES

- (1) Yen, T. F.; Dickie, J. P. Compactness of the aromatic systems in petroleum asphaltics. *J. Inst. Petroleum* **1968**, *54*, 50–53.
- (2) Mullins, O. C. The Modified Yen Model. *Energy Fuels* **2010**, *24*, 2179–2207.
- (3) Dickie, J. P.; Yen, T. F. Macrostructures of the asphaltic fractions by various instrumental methods. *Anal. Chem.* **1967**, *39*, 1847–1852.
- (4) Boduszynski, M. M.; McKay, J. F.; Latham, D. R. Asphaltenes, where are you? *Asphalt Paving Technol.* **1980**, *49*, 123–143.
- (5) Karimi, A.; Qian, K.; Olmstead, W. N.; Freund, H.; Yung, C.; Gray, M. R. Quantitative evidence for bridged structures in asphaltenes by thin film pyrolysis. *Energy Fuels* **2011**, *25*, 3581–3589.
- (6) Gray, M. R.; Tykwinski, R. R.; Stryker, J. M.; Tan, X. Supramolecular assembly model for aggregation of petroleum asphaltenes. *Energy Fuels* **2011**, *25*, 3125–3134.
- (7) Chacón-Patiño, M. L.; Rowland, S. M.; Rodgers, R. P. Advances in Asphaltene Petroleomics. Part 1: Asphaltenes Are Composed of

Abundant Island and Archipelago Structural Motifs. *Energy Fuels* **2017**, *31*, 13509–13518.

(8) Chacón-Patiño, M. L.; Rowland, S. M.; Rodgers, R. P. Advances in Asphaltene Petroleomics. Part 2: Selective Separation Method That Reveals Fractions Enriched in Island and Archipelago Structural Motifs by Mass Spectrometry. *Energy Fuels* **2017**, *32*, 314–328.

(9) Strausz, O. P.; Mojelsky, T. W.; Lown, E. M.; Kowalewski, I.; Behar, F. Structural features of Boscan and Duri asphaltenes. *Energy Fuels* **1999**, *13*, 228–247.

(10) Strausz, O. P.; Peng, P. a.; Murgich, J. About the colloidal nature of asphaltenes and the MW of covalent monomeric units. *Energy Fuels* **2002**, *16*, 809–822.

(11) Acevedo, S.; Gutierrez, L. B.; Negrin, G.; Pereira, J. C.; Mendez, B.; Delolme, F.; Dessalces, G.; Broseta, D. Molecular weight of petroleum asphaltenes: A comparison between mass spectrometry and vapor pressure osmometry. *Energy Fuels* **2005**, *19*, 1548–1560.

(12) Bunger, J. W.; Li, N. C. *Chemistry of Asphaltenes*; American Chemical Society: Washington, DC, 1981.

(13) Buenrostro-Gonzalez, E.; Groenzin, H.; Lira-Galeana, C.; Mullins, O. C. The overriding chemical principles that define asphaltenes. *Energy Fuels* **2001**, *15*, 972–978.

(14) Groenzin, H.; Mullins, O. C. Molecular size and structure of asphaltenes from various sources. *Energy Fuels* **2000**, *14*, 677–684.

(15) Acevedo, S.; Borges, B.; Quintero, F.; Piscitelli, V.; Gutierrez, L. B. Asphaltenes and other natural surfactants from Cerro Negro crude oil. Stepwise adsorption at the water/toluene interface: Film formation and hydrophobic effects. *Energy Fuels* **2005**, *19*, 1948–1953.

(16) Cagna, A.; Esposito, G.; Quinquis, A.-S.; Langevin, D. On the Reversibility of Asphaltene Adsorption at Oil-Water Interfaces. *Colloids Surf., A*, **2018**, ahead of print.54846

(17) Rodgers, R. P.; Schaub, T. M.; Marshall, A. G. Petroleomics: MS returns to its roots. *Anal. Chem.* **2005**, *77*, 20A.

(18) Mullins, O. C.; Sheu, E. Y.; Hammami, A.; Marshall, A. G. *Asphaltenes, Heavy Oils and Petroleomics*; Springer: New York, 2007.

(19) Rodgers, R. P.; Marshall, A. G., *Petroleomics: Advanced Characterization of Petroleum-Derived Materials Characterized by Fourier Transform Ion Cyclotron Resonance Mass Spectrometry (FT-ICR MS)*. In *Asphaltenes, Heavy Oils and Petroleomics*; Mullins, O. C.; Sheu, E. Y.; Hammami, A.; Marshall, A. G., Eds.; Springer: New York, 2007.

(20) Kilpatrick, P. K.; Blankenship, G. A.; Gawrys, K. L. On the distribution of chemical properties and aggregation of solubility fractions in asphaltenes. *Energy Fuels* **2006**, *20*, 705–714.

(21) Klein, G. C.; Angström, A.; Rodgers, R. P.; Marshall, A. G. Use of Saturates/Aromatics/Resins/Asphaltenes (SARA) fractionation to determine matrix effects in crude oil analysis by electrospray ionization Fourier transform ion cyclotron resonance mass spectrometry. *Energy Fuels* **2006**, *20*, 668–672.

(22) Groenzin, H.; Mullins, O. C. Asphaltene molecular size and weight by time-resolved fluorescence depolarization. In *Asphaltenes, Heavy Oils and Petroleomics*; Mullins, O. C.; Sheu, E. Y., Hammami, A., Marshall, A. G., Eds.; Springer: New York, 2007.

(23) Guerra, R. E.; Ladavac, K.; Andrews, A. B.; Mullins, O. C.; Sen, P. N. Diffusivity of coal and petroleum asphaltene monomers by fluorescence correlation spectroscopy. *Fuel* **2007**, *86*, 2016–2020.

(24) Sheu, E. Y.; Long, Y.; Hamza, H. Asphaltene self-association and precipitation in solvents. In *Asphaltenes, Heavy Oils and Petroleomics*; Mullins, O. C.; Sheu, E. Y., Hammami, A., Marshall, A. G., Eds.; Springer: New York, 2007; pp 259–276.

(25) Sirota, E. B.; Lin, M. Y. Physical Behavior of Asphaltenes†. *Energy Fuels* **2007**, *21*, 2809–2815.

(26) Barré, L.; Simon, S.; Palermo, T. Solution properties of asphaltenes. *Langmuir* **2008**, *24*, 3709–3717.

(27) Wang, J.; Li, C.; Zhang, L.; Que, G.; Li, Z. The properties of asphaltenes and their interaction with amphiphiles. *Energy Fuels* **2009**, *23*, 3625–3631.

(28) Sarmah, M. K.; Borthakur, A.; Dutta, A. Pyrolysis of petroleum asphaltenes from different geological origins and use of methyl-naph-

thalenes and methylphenanthrenes as maturity indicators for asphaltenes. *Bull. Mater. Sci.* **2010**, *33*, 509–515.

(29) Ancheyta, J.; Centeno, G.; Trejo, F.; Marroquin, G.; García, J. A.; Tenorio, E.; Torres, A. Extraction and characterization of asphaltenes from different crude oils and solvents. *Energy Fuels* **2002**, *16*, 1121–1127.

(30) Spiecker, P. M.; Gawrys, K. L.; Kilpatrick, P. K. Aggregation and solubility behavior of asphaltenes and their subfractions. *J. Colloid Interface Sci.* **2003**, *267*, 178–193.

(31) Strausz, O. P.; Mojlensky, T. W.; Lown, E. M. The molecular structure of asphaltene: an unfolding story. *Fuel* **1992**, *71*, 1355–1363.

(32) Peng, P. a.; Morales-Izquierdo, A.; Hogg, A.; Strausz, O. P. Molecular structure of Athabasca asphaltene: Sulfide, ether, and ester Linkages. *Energy Fuels* **1997**, *11*, 1171–1187.

(33) Mullins, O. C.; Martinez-Haya, B.; Marshall, A. G. Contrasting Perspective on Asphaltene Molecular Weight: This Comment vs. the Overview of A. A. Herod, K. D. Bartle, and R. Kandiyoti. *Energy Fuels* **2008**, *22*, 1765–1773.

(34) Herod, A. A.; Zhang, S.-F.; Johnson, B. R.; Bartle, K. D.; Kandiyoti, R. Solubility Limitations in the Determination of Molecular Mass Distributions of Coal Liquefaction and Hydrocracking Products: 1-Methyl-2-pyrrolidinone as Mobile Phase in Size Exclusion Chromatography. *Energy Fuels* **1996**, *10*, 743–750.

(35) Akbarzadeh, K.; Hammami, A.; Kharrat, A. M.; Zhang, D.; Allenson, S. J.; Creek, J.; Kabir, S.; Jamaluddin, A. J.; Marshall, A. G.; Rodgers, R. P.; Mullins, O. C.; Solbakken, T. Asphaltenes - Problematic but rich in potential. *Oilfield Rev.* **2007**, 22–43.

(36) Mullins, O. C.; Martinez-Haya, B.; Marshall, A. G. Contrasting Perspective on Asphaltene Molecular Weight. This Comment vs the Overview of A. A. Herod, K. D. Bartle, and R. Kandiyoti. *Energy Fuels* **2008**, *22*, 1765–1773.

(37) Herod, A. A.; Bartle, K. D.; Kandiyoti, R. Comment on a Paper by Mullins, Martinez-Haya, and Marshall “Contrasting Perspective on Asphaltene Molecular Weight. This Comment vs the Overview of A. A. Herod, K. D. Bartle, and R. Kandiyoti”. *Energy Fuels* **2008**, *22*, 4312–4317.

(38) Mullins, O. C. Rebuttal to comment by professors Herod, Kandiyoti, and Bartle on “Molecular size and weight of asphaltene and asphaltene solubility fractions from coals, crude oils and bitumen”. *Fuel* **2007**, *86*, 309–312.

(39) Altgelt, K. H.; Boduszynski, M. M. *Composition and Analysis of Heavy Petroleum Fractions*; CRC Press: New York, NY, 1994.

(40) Boduszynski, M. M. Limitations of average structure determination for heavy ends in fossil fuels. *Liquid Fuels Technol.* **1984**, *2*, 211–232.

(41) Boduszynski, M. M. Composition of heavy petroleum. 1. Molecular weight, hydrogen deficiency, and heteroatom concentration as a function of atmospheric equivalent boiling point up to 1400.degree.F (760.degree.C). *Energy Fuels* **1987**, *1*, 2–11.

(42) Boduszynski, M. M. Composition of heavy petroleum. 2. Molecular characterization. *Energy Fuels* **1988**, *2*, 597–613.

(43) Boduszynski, M. M.; Altgelt, K. H. Composition of Heavy Petroleum. 3. An Improved Boiling Point-Molecular Weight Relation. *Energy Fuels* **1992**, *6*, 68–72.

(44) Boduszynski, M. M.; Altgelt, K. H. Composition of heavy petroleum. 4. Significance of the extended atmospheric equivalent boiling point (AEBP) scale. *Energy Fuels* **1992**, *6*, 72–76.

(45) Herod, A. A.; Kandiyoti, R.; Bartle, K. D. Comment on “Molecular size and weight of asphaltene and asphaltene solubility fractions from coals, crude oils and bitumen” by S. Badre, C. C. Goncalves, K. Norinaga, G. Gustavson and O. C. Mullins; *Fuel* **85** (2006) 1-11. *Fuel* **2006**, *85*, 1950–1951.

(46) Mullins, O. C. Rebuttal to comment by professors Herod, Kandiyoti, and Bartle on “Molecular Size and Weight of Asphaltene and Asphaltene Solubility Fractions from Coals, Crude Oils and Bitumen”. *Fuel* **2007**, *86*, 309–312.

(47) Herod, A. A.; Bartle, K. D.; Kandiyoti, R. Characterization of Heavy Hydrocarbons by Chromatographic and Mass Spectrometric Methods: An Overview. *Energy Fuels* **2007**, *21*, 2176–2203.

(48) Herod, A. A.; Kandiyoti, R. Comment on “Limitations of Size-Exclusion Chromatography in Analyzing Petroleum Asphaltene: A Proof by Atomic Force Microscopy” By M. Behrouzi and P. F. Luckman, Eds., *Energy Fuels*, 2008, *22* (3), 1792-1798, DOI: 10.1021/ef800064q. *Energy Fuels* **2008**, *22*, 4307–4309.

(49) Badre, S.; Carla Goncalves, C.; Norinaga, K.; Gustavson, G.; Mullins, O. C. Molecular size and weight of asphaltene and asphaltene solubility fractions from coals, crude oils and bitumen. *Fuel* **2006**, *85*, 1–11.

(50) Boduszynski, M. M.; Altgelt, K. H. *Composition and Analysis of Heavy Petroleum Fractions*; CRC Press: New York, NY, 1994.

(51) Mullins, O. C.; Sheu, E. Y.; Hammami, A.; Marshall, A. G., Eds.; *Asphaltene, Heavy Oil and Petrochemicals*; Springer: New York, 2007.

(52) Wang, W.; Taylor, C.; Hu, H.; Humphries, K. L.; Jaini, A.; Kitimet, M.; Scott, T.; Stewart, Z.; Ulep, K. J.; Houck, S.; Luxon, A.; Zhang, B.; Miller, B.; Parish, C. A.; Pomerantz, A. E.; Mullins, O. C.; Zare, R. N. Nanoaggregates of diverse asphaltene by mass spectrometry and molecular dynamics. *Energy Fuels* **2017**, *31*, 9140–9151.

(53) McKenna, A. M.; Donald, L. J.; Fitzsimmons, J. E.; Juyal, P.; Spicer, V.; Standing, K. G.; Marshall, A. G.; Rodgers, R. P. Heavy petroleum composition. 3. Asphaltene aggregation. *Energy Fuels* **2013**, *27*, 1246–1256.

(54) Pomerantz, A. E.; Wu, Q.; Mullins, O. C.; Zare, R. N. Laser-based mass spectrometric assessment of asphaltene molecular weight, molecular architecture, and nanoaggregate number. *Energy Fuels* **2015**, *29*, 2833–2842.

(55) McKenna, A. M.; Marshall, A. G.; Rodgers, R. P. Heavy Petroleum Composition. 4. Asphaltene Compositional Space. *Energy Fuels* **2013**, *27*, 1257–1267.

(56) Giraldo-Dávila, D.; Chacón-Patiño, M. L.; McKenna, A. M.; Blanco-Tirado, C.; Combariza, M. Y. Correlations between Molecular Composition and Adsorption, Aggregation, and Emulsifying Behaviors of PetroPhase 2017 Asphaltene and Their Thin-Layer Chromatography Fractions. *Energy Fuels* **2017**, *32*, 2769–2780.

(57) Witt, M.; Godejohann, M.; Oltmanns, S.; Moir, M.; Rogel, E. Characterization of Asphaltene Precipitated at Different Solvent Power Conditions Using Atmospheric Pressure Photoionization (APPI) and Laser Desorption Ionization (LDI) Coupled to Fourier Transform Ion Cyclotron Resonance Mass Spectrometry (FT-ICR MS). *Energy Fuels* **2017**, *32*, 2653–2660.

(58) Giraldo-Dávila, D.; Chacón-Patiño, M. L.; Orrego-Ruiz, J. A.; Blanco-Tirado, C.; Combariza, M. Y. Improving compositional space accessibility in (+) APPI FT-ICR mass spectrometric analysis of crude oils by extrography and column chromatography fractionation. *Fuel* **2016**, *185*, 45–58.

(59) Alvarez-Ramírez, F.; Ruiz-Morales, Y. Island versus archipelago architecture for asphaltene: Polycyclic aromatic hydrocarbon dimer theoretical studies. *Energy Fuels* **2013**, *27*, 1791–1808.

(60) Silva, R. C.; Radović, J. R.; Ahmed, F.; Ehrmann, U.; Brown, M.; Carbognani Ortega, L.; Larter, S.; Pereira-Almao, P.; Oldenburg, T. B. P. Characterization of acid-soluble oxidized asphaltene by Fourier transform ion cyclotron resonance mass spectrometry: Insights on oxycracking processes and asphaltene structural features. *Energy Fuels* **2015**, *30*, 171–179.

(61) Schuler, B.; Meyer, G.; Peña, D.; Mullins, O. C.; Gross, L. Unraveling the Molecular Structures of Asphaltene by Atomic Force Microscopy. *J. Am. Chem. Soc.* **2015**, *137*, 9870–9876.

(62) Alshareef, A. H.; Scherer, A.; Tan, X.; Azyat, K.; Stryker, J. M.; Tykwinski, R. R.; Gray, M. R. Effect of chemical structure on the cracking and coking of archipelago model compounds representative of asphaltene. *Energy Fuels* **2012**, *26*, 1828–1843.

(63) Rueda-Velásquez, R. I.; Freund, H.; Qian, K.; Olmstead, W. N.; Gray, M. R. Characterization of Asphaltene Building Blocks by

Cracking under Favorable Hydrogenation Conditions. *Energy Fuels* **2012**, *27*, 1817–1829.

(64) Wang, J.; Anthony, E. J. A study of thermal-cracking behavior of asphaltenes. *Chem. Eng. Sci.* **2003**, *58*, 157–162.

(65) Chacón-Patiño, M. L.; Blanco-Tirado, C.; Orrego-Ruiz, J. A.; Gómez-Escudero, A.; Combariza, M. Y. Tracing the compositional changes of asphaltenes after hydroconversion and thermal cracking processes by high-resolution mass spectrometry. *Energy Fuels* **2015**, *29*, 6330–6341.

(66) Gray, M. R. Consistency of asphaltene chemical structures with pyrolysis and coking behavior. *Energy Fuels* **2003**, *17*, 1566–1569.

(67) Chacón-Patiño, M. L.; Rowland, S. M.; Rodgers, R. P. Advances in Asphaltene Petroleomics. Part 3. Dominance of island or archipelago structural motif is sample dependent. *Energy Fuels* **2018**, *32*, 9106–9120.

(68) Behar, F.; Lorant, F.; Mazeas, L. Elaboration of a new compositional kinetic schema for oil cracking. *Org. Geochem.* **2008**, *39*, 764–782.

(69) Wiehe, I. A. The pendant-core building block model of petroleum residua. *Energy Fuels* **1994**, *8*, 536–544.

(70) Jaffe, S. B.; Freund, H.; Olmstead, W. N. Extension of structure-oriented lumping to vacuum residua. *Ind. Eng. Chem. Res.* **2005**, *44*, 9840–9852.

(71) Zhao, Y.; Gray, M. R.; Chung, K. H. Molar kinetics and selectivity in cracking of Athabasca asphaltenes. *Energy Fuels* **2001**, *15*, 751–755.

(72) Speight, J. *Handbook of Petroleum Analysis*; John Wiley & Sons, 2001; pp 232–233.

(73) Speight, J. G. Petroleum Asphaltenes - Part 1: Asphaltenes, Resins and the Structure of Petroleum. *Oil and Gas Science and Technology* **2006**, *59*, 467–477.

(74) Baker, E. W. Mass Spectrometric Characterization of Petroporphyrins I. *J. Am. Chem. Soc.* **1966**, *88*, 2311.

(75) Baker, E. W.; Yen, T. F.; Dickie, J. P.; Rhodes, R. E.; Clark, L. F. Mass spectrometry of porphyrins. II. Characterization of petroporphyrins. *J. Am. Chem. Soc.* **1967**, *89*, 3631–3639.

(76) Xu, H.; Lesage, S. Separation of vanadyl and nickel petroporphyrins on an aminopropyl column by high-performance liquid chromatography. *J. Chromatogr. A* **1992**, *607*, 139–144.

(77) Ocampo, R.; Riva, A.; Trendel, J. M.; Riolo, J.; Callot, H. J.; Albrecht, P. Petroporphyrins as biomarkers in oil-oil and oil-source rock correlations. *Energy Fuels* **1993**, *7*, 191–193.

(78) Qian, K.; Edwards, K. E.; Mennito, A. S.; Walters, C. C.; Kushnerick, J. D. Enrichment, Resolution, and Identification of Nickel Porphyrins in Petroleum Asphaltene by Cyclograph Separation and Atmospheric Pressure Photoionization Fourier Transform Ion Cyclotron Resonance Mass Spectrometry. *Anal. Chem.* **2010**, *82*, 413–419.

(79) Putman, J. C.; Rowland, S. M.; Corilo, Y. E.; McKenna, A. M. Chromatographic enrichment and subsequent separation of nickel and vanadyl porphyrins from natural seeps and molecular characterization by positive electrospray ionization FT-ICR mass spectrometry. *Anal. Chem.* **2014**, *86*, 10708–10715.

(80) McKenna, A. M.; Blakney, G. T.; Xian, F.; Glaser, P. B.; Rodgers, R. P.; Marshall, A. G. Heavy Petroleum Composition. 2. Progression of the Boduszynski Model to the Limit of Distillation by Ultrahigh-Resolution FT-ICR Mass Spectrometry. *Energy Fuels* **2010**, *24*, 2939–2946.

(81) Jewell, D. M.; Ruberto, R. G.; Davis, B. E. Systematic Approach to the Study of Aromatic Hydrocarbons in Heavy Distillates and Residues by Elution Adsorption Chromatography. *Anal. Chem.* **1972**, *44*, 2318–2321.

(82) Jewell, D. M.; Weber, J. H.; Bunger, J. W.; Plancher, H.; Latham, D. R. Ion-Exchange, Coordination, and Adsorption Chromatographic Separation of Heavy-End Petroleum Distillates. *Anal. Chem.* **1972**, *44*, 1391–1395.

(83) Chacón-Patiño, M. L.; Vesga-Martínez, S. J.; Blanco-Tirado, C.; Orrego-Ruiz, J. A.; Gómez-Escudero, A.; Combariza, M. Y. Exploring Occluded Compounds and Their Interactions with Asphaltene

Networks Using High-Resolution Mass Spectrometry. *Energy Fuels* **2016**, *30*, 4550–4561.

(84) Emmett, M. R.; White, F. M.; Hendrickson, C. L.; Shi, S. D.-H.; Marshall, A. G. Application of micro-electrospray liquid chromatography techniques to FT-ICR MS to enable high-sensitivity biological analysis. *J. Am. Soc. Mass Spectrom.* **1998**, *9*, 333–340.

(85) Kaiser, N. K.; Quinn, J. P.; Blakney, G. T.; Hendrickson, C. L.; Marshall, A. G. A Novel 9.4 Tesla FTICR Mass Spectrometer with Improved Sensitivity, Mass Resolution, and Mass Range. *J. Am. Soc. Mass Spectrom.* **2011**, *22*, 1343–1351.

(86) Hendrickson, C. L.; Quinn, J. P.; Kaiser, N. K.; Smith, D. F.; Blakney, G. T.; Chen, T.; Marshall, A. G.; Weisbrod, C. R.; Beu, S. C. 21 Tesla Fourier transform ion cyclotron resonance mass spectrometer: A national resource for ultrahigh resolution mass analysis. *J. Am. Soc. Mass Spectrom.* **2015**, *26*, 1626–1632.

(87) Smith, D. F.; Podgorski, D. C.; Rodgers, R. P.; Blakney, G. T.; Hendrickson, C. L. 21 Tesla FT-ICR Mass Spectrometer for Ultrahigh-Resolution Analysis of Complex Organic Mixtures. *Anal. Chem.* **2018**, *90*, 2041–2047.

(88) Kaiser, N. K.; Savory, J. J.; Hendrickson, C. L. Controlled ion ejection from an external trap for extended m/z range in FT-ICR mass spectrometry. *J. Am. Soc. Mass Spectrom.* **2014**, *25*, 943–949.

(89) Kaiser, N. K.; McKenna, A. M.; Savory, J. J.; Hendrickson, C. L.; Marshall, A. G. Tailored ion radius distribution for increased dynamic range in FT-ICR mass analysis of complex mixtures. *Anal. Chem.* **2012**, *85*, 265–272.

(90) Chen, T.; Beu, S. C.; Kaiser, N. K.; Hendrickson, C. L. Note: Optimized circuit for excitation and detection with one pair of electrodes for improved Fourier transform ion cyclotron resonance mass spectrometry. *Rev. Sci. Instrum.* **2014**, *85*, 0666107/1–0666107/3.

(91) Tolmachev, A. V.; Robinson, E. W.; Wu, S.; Kang, H.; Lourette, N. M.; Paša-Tolić, L.; Smith, R. D. Trapped-Ion Cell with Improved DC Potential Harmonicity for FT-ICR MS. *J. Am. Soc. Mass Spectrom.* **2008**, *19*, 586–597.

(92) Kaiser, N. K.; Savory, J. J.; McKenna, A. M.; Quinn, J. P.; Hendrickson, C. L.; Marshall, A. G. Electrically compensated Fourier transform ion cyclotron resonance cell for complex mixture mass analysis. *Anal. Chem.* **2011**, *83*, 6907–6910.

(93) Boldin, I. A.; Nikolaev, E. N. Fourier transform ion cyclotron resonance cell with dynamic harmonization of the electric field in the whole volume by shaping of the excitation and detection electrode assembly. *Rapid Commun. Mass Spectrom.* **2010**, *25*, 122–126.

(94) Blakney, G. T.; Hendrickson, C. L.; Marshall, A. G. Predator data station: A fast data acquisition system for advanced FT-ICR MS experiments. *Int. J. Mass Spectrom.* **2011**, *306*, 246–252.

(95) Xian, F.; Hendrickson, C. L.; Blakney, G. T.; Beu, S. C.; Marshall, A. G. Automated Broadband Phase Correction of Fourier Transform Ion Cyclotron Resonance Mass Spectra. *Anal. Chem.* **2010**, *82*, 8807–8812.

(96) Savory, J. J.; Kaiser, N. K.; McKenna, A. M.; Xian, F.; Blakney, G. T.; Rodgers, R. P.; Hendrickson, C. L.; Marshall, A. G. Parts-Per-Billion Fourier Transform Ion Cyclotron Resonance Mass Measurement Accuracy with a “Walking” Calibration Equation. *Anal. Chem.* **2011**, *83*, 1732–1736.

(97) Kendrick, E. A mass scale based on $\text{CH}_2 = 14.0000$ for high resolution mass spectrometry of organic compounds. *Anal. Chem.* **1963**, *35*, 2146–2154.

(98) Hughey, C. A.; Hendrickson, C. L.; Rodgers, R. P.; Marshall, A. G.; Qian, K. Kendrick Mass Defect Spectrum: A Compact Visual Analysis for Ultrahigh-Resolution Broadband Mass Spectra. *Anal. Chem.* **2001**, *73*, 4676–4681.

(99) McLafferty, F. W.; Turecek, F. *Interpretation of Mass Spectra*, 4th ed.; University Science Books: Mill Valley, CA, 1993.

(100) Corilo, Y. E. *PetroOrg Software*; Florida State University, Omics LLC: Tallahassee, FL, 2014.

(101) McKenna, A. M.; Purcell, J. M.; Rodgers, R. P.; Marshall, A. G. Heavy petroleum composition. 1. Exhaustive compositional analysis of Athabasca bitumen HVGO distillates by Fourier transform ion

cyclotron resonance mass spectrometry: a definitive test of the Boduszynski model. *Energy Fuels* **2010**, *24*, 2929–2938.

(102) Frakman, Z.; Ignasiak, T. M.; Montgomery, D. S.; Strausz, O. P. Nitrogen compounds in Athabasca asphaltene: The vanadyl porphyrins. *AOSTRA J. Res.* **1988**, *4*, 171–179.

(103) Li, N.; Ma, X.; Zha, Q.; Song, C. Analysis and comparison of nitrogen compounds in different liquid hydrocarbon streams derived from petroleum and coal. *Energy Fuels* **2010**, *24*, 5539–5547.

(104) Zeuthen, P.; Knudsen, K. G.; Whitehurst, D. D. Organic nitrogen compounds in gas oil blends, their hydrotreated products and the importance to hydrotreatment. *Catal. Today* **2001**, *65*, 307–314.

(105) Zhu, X.; Shi, Q.; Zhang, Y.; Pan, N.; Xu, C.; Chung, K. H.; Zhao, S. Characterization of Nitrogen Compounds in Coker Heavy Gas Oil and Its Subfractions by Liquid Chromatographic Separation Followed by Fourier Transform Ion Cyclotron Resonance Mass Spectrometry. *Energy Fuels* **2011**, *25*, 281–287.

(106) Purcell, J. M.; Rodgers, R. P.; Hendrickson, C. L.; Marshall, A. G. Speciation of nitrogen containing aromatics by atmospheric pressure photoionization or electrospray ionization Fourier transform ion cyclotron resonance mass spectrometry. *J. Am. Soc. Mass Spectrom.* **2007**, *18*, 1265–1273.

(107) Purcell, J. M.; Hendrickson, C. L.; Rodgers, R. P.; Marshall, A. G. Atmospheric Pressure Photoionization Proton Transfer for Complex Organic Mixtures Investigated by Fourier Transform Ion Cyclotron Resonance Mass Spectrometry. *J. Am. Soc. Mass Spectrom.* **2007**, *18*, 1682–1689.

(108) Podgorski, D. C.; Corilo, Y. E.; Nyadong, L.; Lobodin, V. V.; Bythell, B. J.; Robbins, W. K.; McKenna, A. M.; Marshall, A. G.; Rodgers, R. P. Heavy petroleum composition. 5. Compositional and structural continuum of petroleum revealed. *Energy Fuels* **2013**, *27*, 1268–1276.

(109) Smith, D. F.; Rahimi, P.; Teclemariam, A.; Rodgers, R. P.; Marshall, A. G. Characterization of Athabasca Bitumen Heavy Vacuum Gas Oil Distillation Cuts by Negative/Positive Electrospray Ionization and Automated Liquid Injection Field Desorption Ionization Fourier Transform Ion Cyclotron Resonance Mass Spectrometry. *Energy Fuels* **2008**, *22*, 3118–3125.

(110) Li, Y.; Han, S.; Lu, Y.; Zhang, J. Influence of asphaltene polarity on crystallization and gelation of waxy oils. *Energy Fuels* **2018**, *32*, 1491–1497.

(111) Skartlien, R.; Simon, S.; Sjöblom, J. DPD molecular simulations of asphaltene adsorption on hydrophilic substrates: Effects of polar groups and solubility. *J. Disp. Sci. Tech.* **2015**, *37*, 866–883.

(112) Chen, Q.; Gray, M. R.; Liu, Q. Irreversible adsorption of asphaltenes on Kaolinite: Influence of dehydroxylation. *Energy Fuels* **2017**, *31*, 9328–9336.

(113) Hsu, C. S.; Lobodin, V. V.; Rodgers, R. P.; McKenna, A. M.; Marshall, A. G. Compositional boundaries for fossil hydrocarbons. *Energy Fuels* **2011**, *25*, 2174–2178.

(114) Lobodin, V. V.; Marshall, A. G.; Hsu, C. S. Compositional space boundaries for organic compounds. *Anal. Chem.* **2012**, *84*, 3410–3416.

(115) Sullivan, R. F.; Boduszynski, M. M.; Fetzer, J. C. Molecular transformations in hydrotreating and hydrocracking. *Energy Fuels* **1989**, *3*, 603–612.